

N71-33102

NASA TECHNICAL
MEMORANDUM

NASA TM X-62,064

NASA TM X-62,064

PRELIMINARY STUDIES OF THE OXIDATION OF TD Ni-20Cr IN STATIC,
FLOWING, AND DISSOCIATED OXYGEN AT 1100°C AND 130 Nm⁻²

William P. Gilbreath

Ames Research Center
Moffett Field, Calif. 94035

August 1971

PRELIMINARY STUDIES OF THE OXIDATION OF TD Ni-20Cr IN STATIC,
FLOWING, AND DISSOCIATED OXYGEN AT 1100°C AND 130 Nm⁻²

by

William P. Gilbreath

Abstract

The degradation behavior of a candidate space shuttle TPS material, TD NiCr, is examined at 1100°C (2000°F) in three oxygen environments at a pressure of 130 Nm⁻² (1 torr): static molecular oxygen, flowing molecular oxygen, and flowing atomic oxygen. The last environment, of the three, provides the most reasonable simulation of shuttle orbital vehicle reentry, during oxidation; it also produces several interesting phenomena not normally seen in molecular oxygen. In atomic oxygen, TD NiCr volatilizes faster, has a faster rate of oxide growth, and greater metal recession than occurs in molecular oxygen. The oxide scale formed in atomic oxygen is essentially devoid of chromium and it has a high-temperature emittance that is significantly lower than from the oxides formed in molecular oxygen. In view of these preliminary findings, all candidate shuttle TPS materials are being re-examined to determine their behavior in a dissociated oxygen environment in order to better assess their real usefulness as skin materials for this mission.

INTRODUCTION

The space shuttle concept, because of the reusability requirement for more than one hundred launches and reentries for a single vehicle, poses complex materials problems, particularly for the outer (TPS) skin of the orbital vehicle. The survivability of single-reentry vehicles from orbit is, of course, well within present materials technology for vehicles utilizing ablative heat shields in high-heating areas. However, utilization of these skin materials for the shuttle orbital vehicle would in most cases be limited because they would require replacement for subsequent flights. As it is not feasible to test materials proposed for multiple reentries under actual flight conditions, it is important to adequately simulate the reentry environment in the laboratory if accurate predictions of material behavior in shuttle usage are to be made. Prediction of the oxidation resistance of a given shuttle candidate material can be in error if the actual reentry environment-material interaction differs from that predicted from laboratory simulation. It is the purpose of

this report to present preliminary results of oxidation tests, under various simulated reentry conditions, on one of the leading candidate shuttle TPS materials--a thoria-dispersed-nickel, 20% chromium alloy (TD NiCr). These tests clearly illustrate the necessity for better understanding of how to test materials in order to correctly predict behavior during entry.

TD NiCr (and the whole family of alloys with these basic components) is one of the major candidates for use on the space shuttle on surfaces expected to experience service temperatures between 1000 and 1200°C (1800 to 2200°F). A few studies have been made on the oxidation resistance of TD NiCr in this temperature regime. Goldstein¹ has developed an analytical model for the "ablation" of this alloy under hypervelocity oxidation conditions and Centolanzi² has reported the results of arc-jet oxidation on this material. Both of these authors, as well as others, have pointed out differences between results of static and flowing gas studies on this material. A study by Kohl and Stearns³ calculated, under static conditions, theoretical rates of volatilization of TD NiCr as a function of temperature and oxygen and water partial pressure, as derived from thermodynamic considerations. Goward⁴ compared the oxidation properties of TD NiCr with other superalloys. Giggins and Pettit⁵ have recently reported on the oxidation behavior of TD NiCr between 900 and 1200°C in static oxygen at 10^4 Nm^{-2} (0.1 atm). In addition, a large number of experimental oxidation studies have been performed with NiCr alloys (not dispersion strengthened) of various compositions as a function of temperature and oxygen pressure.

Figure 1 shows a calculated altitude-environment diagram for a shuttle-configured vehicle entering Earth's atmosphere at 30° angle of attack. Much of the information presented in this figure has been derived from a report by Stine.⁶ This figure indicates that during a crucial part of reentry, when the vehicle TPS materials are experiencing maximum design temperatures (1000 - 1200°C for the TD NiCr), a large fraction of the boundary layer oxygen is dissociated. It should be recognized that, although at altitudes above 90 km the dissociation may not reach completion until hundreds of feet downstream of the shockwave,⁶ the immediate environment of the vehicle still contains significant amounts of oxygen atoms since the oxygen in the free stream is about 5% dissociated at 90 km and 50% at 120 km.⁷ Since for most materials the rate of attack by atomic oxygen is much greater than that by molecular oxygen^{8,9} and since the reentry environment contains large quantities of atomic oxygen, it is essential that candidate TPS materials be examined for compatibility with dissociated oxygen. Reaction with atomic oxygen is essentially not thermally activated and, thus, all atoms that reach the surface of the material are capable of reaction. The literature apparently contains no information on the specific reaction of atomic oxygen with either NiCr or TD NiCr alloys. Information⁹ on the attack of nickel by atomic oxygen indicates that, at least under certain conditions, the oxidation rate is enhanced by about a factor of ten over that observed in molecular oxygen.

EXPERIMENTAL APPROACH

Experiments were carried out on TD NiCr in environments of static molecular oxygen, flowing molecular oxygen, and flowing atomic oxygen. Two types of apparatus were used in the experiments. In one apparatus, (Figure 2) a 1.2x10x0.05 cm specimen was suspended, in a quartz tube, by means of a platinum wire from a auto-recording vacuum balance. Specimens were radiantly heated by an external quartz-lamp furnace. In the other apparatus (Figure 3), a 0.9x5x0.025 cm specimen was end mounted in a liquid-nitrogen-cooled copper jig and resistively heated inside of a quartz tube. The specimens were cut from large panels and used, except for an acetone and ethanol degrease, in the as-recieved condition.

In the radiantly-heated apparatus, operating temperatures were derived from the lamp power settings and optical pyrometer sightings, which were both previously calibrated against a Pt/Pt-10% Rh thermocouple attached to "dummy" specimens of the same material suspended in place. The resistively heated specimens had a Pt/Pt-10% Rh thermocouple spot welded to the center of the back (i.e., away from the flow), while a pyrometer (Huggins Labs Model 31C00 infrascopes) measured emittance and temperature uniformity ($\pm 15^{\circ}\text{C}$ over 90% of the sample, greater deviation occurred at the cooled grips which were near the ends).

Atomic oxygen was generated by means of a tunable, air-cooled, microwave cavity surrounding the quartz tube and powered by a 100-watt microwave generator. For the radiantly-heated specimen, this meant that the atomic oxygen was generated approximately 8 cm upstream (in order for the cavity to be outside the radiant heater) and, at the pressure level used, a large fraction of the dissociated oxygen had recombined before reaching the specimen so that only part of the specimen was exposed to an appreciable but unmeasured atomic oxygen flux (as evidenced, in part, by disappearance of the "glow" in the stream). For the resistively-heated specimen, the cavity was placed directly around the sample and thus exposed it to a large dissociated fraction (about 0.4, see ref. 10).

All experiments were performed at an oxygen pressure of about 130 Nm^{-2} as measured by a calibrated thermocouple gage. The "static" tests were made either by replacing the oxygen after each heating interval or by making the tests in slowly ($< 0.05 \text{ m sec}^{-1}$) flowing oxygen. All flow tests (both in atomic and molecular oxygen) were made at flow velocities of 12 m sec^{-1} at the specimen parallel to the length of the sample on the balance and directed head-on at the exterior base of the U-shaped, resistively-heated specimen. All tests were performed at 1100°C (2000°F), the proposed intermediate service temperature of TD NiCr, under cyclic heating conditions comprised of heating intervals of 1 to 10 ks interrupted by cooling periods of about 500 seconds. The specimens were weighed prior to oxidation (with thermocouple attached

the case of the resistively-heated specimens); then they were weighed after each heating interval for the specimens suspended from the balance and after completion of the experiment for the specimens resistively-heated (following 10 to 40 ks of heating). In addition to the weight-change measurements, the emittance of the specimens was determined and, after oxidation, the specimens were examined by light-microscope, scanning-electron microscope, and electron-microprobe means.

OXIDATION RESULTS AND DISCUSSION

Weight Change

Radiantly Heated Specimens:

Figure 4 shows that the oxidation of TD NiCr, as determined with thermogravimetry in the apparatus of Figure 2, exhibited quite different behavior in each environment. Under the conditions given for the static oxidation experiments, TD NiCr was found to oxidize in a manner typical of that reported⁶ for NiCr alloys. The parabolic rate constant, K_p , derived from the data shown is $1.0 \times 10^{-12} \text{ g}^2 \text{ cm}^{-4} \text{ s}^{-1}$. This compares well with the K_p calculated (for the early stages of oxidation) by Giggins and Pettit.⁵ In all cases for flowing molecular oxygen and under the conditions noted, an initial weight gain was exhibited followed by a gradual weight loss. The weight-loss rate in the flowing molecular oxygen environments was about 10% of the theoretical vaporization rate of $8 \times 10^{-8} \text{ g cm}^{-2} \text{ s}^{-1}$ calculated by Kohl and Stearns.³ Several possible explanations exist for the discrepancy. The experimental rates found are overall rates include the creation of more sample mass through the formation of non-volatile NiO and Cr_2O_3 , which was not included in the theoretical calculation of ref. 3. Further, the determined rates may be diffusion limited if either insufficient mixing occurs at the gas-metal interface (a likely probability, at least, in the static experiments) or if chromium transport is blocked by Ni, or NiO, or ThO_2 (see ref. 5). Finally, the calculations of Kohl and Stearns neglect any effect the dispersed thorium might have on the vaporization process. In the case of the oxidation of TD NiCr by atomic oxygen, an almost constant rate of weight decrease in the specimens was found—the rate of loss was about three times that caused by flowing molecular oxygen. Since (as noted above) the oxygen-atom concentration was dilute at the bottom of the specimen and probably non-existent at the upper portions of the specimen, it is not possible to draw quantitative results from these latter data. This point will be further discussed below in conjunction with other results on the oxides formed.

Changes in the duration of the heating and cooling cycles had no apparent effect on the overall weight changes noted. The cumulative heating time was the prime factor as all data fell on fairly smooth

curves regardless of the length of a given heating cycle. Further, whether or not the specimens were brought to a normal atmospheric pressure of air between heating cycles seemed to make no difference in the weight changes observed.

Aside from the evidence given by the weight loss, volatilization of the alloy in the flowing gas experiments was also apparent by condensation of a product(s) on the interior of the clear quartz tube which surrounded the heated specimen. Virtually from the start of heating, in the flowing atomic oxygen experiments, a red-brown deposit began forming on the upper, cooler surface of the tube and, after a couple hours, a similar phenomenon was noted in flowing molecular oxygen. In both environments, a green deposit began forming, after several hours of heating, on the hottest area of the tube—that adjacent to the specimen. The red-brown deliquescent condensate on the cooler portion of the tube was identified as chromium trioxide (CrO_3) by microprobe analysis and by virtue of its water solubility. The green condensate was also composed of chromium and, based on its color and acid/alkaline insolubility, it was identified as the sesquioxide (Cr_2O_3). Since this latter oxide is not volatile³ under the experimental conditions, it was assumed to be a reaction product of one of the volatile chromium oxides (either CrO_3 or CrO_2) with the hot quartz. For the static tests, no discoloration of the tube was observed - which implies that no volatilization takes place under that condition.

Resistively Heated Specimens:

For the specimens resistively heated (Figure 3), a rough measure of the overall weight-change characteristics of TD NiCr was found by determining the difference between pre- and post-oxidation weights. In static oxygen, the one specimen tested gained about 0.5 mg cm^{-2} in ten hours, about the same increase as for the static experiments shown in Figure 4. In flowing atomic oxygen for three specimens oxidized, for periods of 3, 6, and 10 hours, small, erratic weight changes were found. A large quantity of the red-brown condensate (CrO_3) collected downstream from the specimen and a relatively thick oxide coating formed on these specimens. The differences in weight-change results given here from those in Figure 4 for TD NiCr in atomic oxygen will be discussed below.

Post-Oxidation Examination

The specimens oxidized by molecular oxygen had dark grey or black coloration while, in general, the specimens exposed to dissociated oxygen were brightly colored. A description of the visual appearance of typical specimens along with an electron microprobe analysis of particular areas is given in Table I. For the microprobe analysis, the interior of an

unoxidized specimen was assumed to be a standard 78% nickel and 20% chromium, by weight. Counts on the oxidized specimens were related to the standard to determine the percent chromium and nickel in the mixed oxide. These values are reported in Table I as the oxides - assuming nickel to be present solely as NiO and chromium as Cr_2O_3 . The near-unity total for each analysis indicates that these assumptions are probably valid. For molecular oxygen, at least, these two oxides along with the spinel, NiCr_2O_4 (which would not affect the above approach), are the only oxides expected.^{5,11} For oxygen-atom oxidation, the results of two types of experiment are shown: (1) a specimen on the balance (Figure 2) which shows the effects of decrease in atomic oxygen concentration in going from the whitish to the dark areas (grey areas with black streaks covered the upper three-quarters of the specimen) and (2) a specimen heated resistively (Figure 3) and completely immersed in atomic oxygen which developed a yellow coloration on the side toward the flow and a green coloration in a relatively stagnant area on the back side of the specimen.

The nearly pure Cr_2O_3 surface scale formed in the static experiment (Table I) is expected^{4,5,11} and is indicative of the oxidation resistance mechanism observed for normal oxidation of NiCr alloys. The smaller amounts of Cr_2O_3 found in the other oxidation experiments are due to vaporization of chromium as CrO_3 and also indicate that these specimens are relatively less resistant to further oxidation. The higher concentrations of NiO appear to be associated with the more brightly colored areas.

One of the important characteristics of an oxidation resistant (or protective) oxide is its degree of adherence to the substrate. In the handling of the oxidized specimens, some purely qualitative observations were made. The yellow and green oxides formed on the atomically oxidized specimens had very low adherence, compared to the black or grey oxides. A sharp tap removed much of the yellow oxide - a dry powder - while the green material could be scraped from the surface as a coherent mass. Beneath the green and yellow oxides was an adherent dark substrate oxide.

To derive a further indication of the relative degree of degradation in the three environments, the magnitude of metal recession and oxide thickness was measured in several instances, and the results are presented in Table II. The values were obtained from photomicrographs of cross-sectioned specimens (except for the static oxidized specimen for which the values shown were calculated from the weight gain data) and are for a single surface. These data indicate that atomic oxygen attacks TD NiCr at least several times faster than molecular oxygen and leads to enhanced oxide formation.

The data presented above and the results of other investigations (e.g. ref. 1) indicate that, in all test environments studied, two

competing processes are taking place: metal oxidation to form NiO and Cr₂O₃ and subsequent volatilization of the Cr₂O₃ as CrO₃. Goldstein¹ showed, in static oxygen (or air), that although sufficient oxygen might reach the TD NiCr surface for oxidation, transport of CrO₃ away from the surface was so slow that it effectively limited vaporization. Thus, the parabolic-weight-gain oxidation kinetics noted in Figure 4 can be explained. The flowing oxygen results (Figure 4) indicate that metal oxidation and CrO₃ volatilization occur continuously and cause the long-term weight change behavior noted. The overall attack (as judged by metal recession and oxide formation, Table II) is greater in the flowing gas case since loss of chromium leaves the nickel relatively unprotected. A dilute oxygen-atom concentration (Figure 4) apparently caused even greater volatilization with associated changes in composition, metal recession and oxidation rate (Tables I and II). At high oxygen-atom concentrations (40%), the substrate weight gain (due principally to NiO formation) apparently balanced the weight loss from volatilization of CrO₃. Alloy degradation (as evidenced by increased oxide thickness and metal recession) was about two orders of magnitude greater in atomic oxygen than in static oxygen and about one order greater than caused by flowing molecular oxygen. It should be noted that volatilization may be limited by rate of oxygen flow, by rate of diffusion of CrO₃ through the nickel-oxide scale, and boundary layer or by the vapor pressure of CrO₃.

Arc-jet testing provides a separate means of examining shuttle TPS materials under simulated conditions of pressure, temperature, and flow rate. Although the arc-jet produces an environment high in ionized oxygen and low in atomic oxygen (relative to the shuttle orbital vehicle reentry environment) it is considered^{1,2,6} to provide a better reentry simulation than static or ordinary flowing molecular gas studies. Although the flowing atomic-oxygen tests described above simulate the species and temperature environment, they are up to a decade low in oxygen partial pressure and in a much different flow environment; thus, it is difficult, at least at this time, to meaningfully and quantitatively compare the test results from the above atomic-oxygen experiments with either the arc-jet results or the expected atmosphere-entry itself. However, the overall attack rate in atomic oxygen is the same order as that given by Centolanzi² for arc-jet degradation of TD NiCr.

High Temperature Emittance Properties

For both design and protective purposes for radiation heat shields, it is important that a given TPS material maintain a stable high emittance during its service life. Therefore, approximate measurements of the emittance of the specimens have also been made after oxidation in the various test environments. The pyrometer used to monitor specimen temperature has a feature which permits adjustments to be made for sample

emittance. Thus, in an approximate manner, it was possible to measure either relative emittances between portions of a sample held at a uniform temperature or to measure "normal" emittance (at the wavelengths for which the pyrometer was designed) if a primary measurement of the temperature was possible (as by thermocouple). The high-temperature emittances given in Table III were determined by these means for radiation between 1.8 and 2.5 μ (the pyrometer bandpass). The measured differences in emittance between the surfaces of TD NiCr oxidized in molecular and atomic oxygen are significant. The yellow surface at, say, $\epsilon = 0.75$ must be 55°C hotter than the black surface, $\epsilon = 0.88$, at 1100° C to radiate equivalent amounts of thermal energy. If the TD NiCr were expected to operate at the maximum service temperature of 1200°C at a planned emittance of 0.88, formation of an adherent yellow oxide with its lower emittance would severely shorten the service life. However, the poor adherence of the yellow oxide, as described earlier, may preclude its building up a coating during the rigors of flight sufficient to cause a reduction in emittance.

CONCLUDING REMARKS

The results of a preliminary study on the oxidation of TD NiCr comparing the effects of atomic and molecular oxygen have been presented. It was shown that, for a critical portion of the reentry of the shuttle vehicle, it will be under attack by dissociated oxygen and, thus, candidate shuttle TPS materials should be examined for their resistance toward this species. One candidate shuttle material, TD NiCr, was found to deteriorate considerably more rapidly in flowing atomic oxygen than in either static or flowing molecular oxygen. This was especially evidenced by the enhanced vaporization and the thicker oxide scale formation which occurred in atomic oxygen. Another possible problem occurring because of exposure to atomic oxygen was the lowering of surface emittance due to the formation of a yellow nickel oxide (rather than a black oxide as formed in molecular oxygen).

Much further work is indicated in this area. The present program will be extended to other temperatures, and the effects of various pressures, oxygen-atom concentrations, and flow velocities will be examined. It is hoped that from this information the degradation mechanisms can be determined. A program has also been initiated to investigate the changes in mechanical properties of TD NiCr which may result from the chemical attack in the three environments. A number of other candidate shuttle TPS materials will also be investigated to determine their behavior when subject to atomic oxygen attack.

REFERENCES

1. Goldstein, Howard E.: "An Analytical Model for Hypersonic Ablation of Thoria Dispersed Nickel Chromium Alloy". AIAA Paper 71-34, AIAA 9th Aerospace Sciences Meeting, January 25-27, 1971.
2. Centolanzi, Frank J.: "Hypervelocity Oxidation Tests of Thoria Dispersed Nickel Chromium Alloys". NASA TMX-62,015.
3. Kohl, Fred J., and Stearns, Carl A.: "Vaporization of Chromium Oxides from the Surface of TD-NiCr under Oxidizing Conditions" NASA TMX-52879, August, 1970.
4. Goward, G. W.: "Current Research on the Surface Protection of Superalloys for Gas Turbine Engines". J. Metals, pp. 31-39, 1970.
5. Giggins, C. S. and Pettit, F. S.: "The Oxidation of TD NiC (Ni-20Cr-2vol pct ThO₂) Between 900° and 1200°C". Met. Trans. Vol. 2, pp. 1071-1078, April, 1971.
6. Stine, Howard A.: "Effects of Surface Catalysis on Heat Transfer to Shuttle Orbiter". NASA TMX-62,016. March, 1971.
7. Johnson, Francis S.: "Satellite Environment Handbook". 2nd Edition, Stanford University, 1965.
8. Rosner, Daniel E., and Allendorf, H. Donald: "Kinetic Studies of the attack of Refractory Materials by Oxygen Atoms and Chlorine Atoms". High Temperature Technology, Butterworths 1967, pp. 707-719.
9. Dickens, P. G., Heckingbottom, R., and Linnett, J. W.: "Oxidation of Metals and Alloys, Part II. Trans. Far. Soc. Vol. 65, pp. 2235-2247, 1969.
10. Brown, Robert L.: Effects of Impurities on the Production of Oxygen Atoms by a Microwave Discharge". Journ. Phys. Chem. Vol. 71, pp. 2492-2495, 1967.
11. Tribbeck, T. D., Linnett, J. W., and Dickens, P. G.: "Oxidation of Metals and Alloys, Part I". Trans. Far. Soc. V. 65, pp. 890-895, 1969.

TABLE I

Surface Characterization of Oxidized TD NiCr

Test Condition (all 1100°C and 130 Nm ⁻²)	Location	Color	Analysis as Molecular %	
			Cr ₂ O ₃	NiO
<u>Radiative Heating</u>				
Static O ₂ , 50 ks	Intermixed	Charcoal Shiny black	99	1
			87	8
Flowing O ₂ , 70 ks	Intermixed	Grey Black	54	49
			81	23
Flowing 0+0 ₂ ,	Upstream	Whitish	45	53
	↓	Yellow over green	7	92
		Green	47	50
		Black nodules	50	52
		Black	95	2
	Downstream	Grey	70	29
<u>Resistive Heating</u>				
Flowing 0+0 ₂ , 10 ks	Upstream	Yellow-grey	25	73
	Downstream	Green	56	45

TABLE II

Metal Recession and Oxide Thickness of Oxidized TD NiCr

Test Condition (all 1100°C and 130 Nm ⁻²)	Metal Recession (cm)	Oxide Thickness (cm)
<u>Radiative heating</u>		
Static O ₂ , 35 ks	0.00003	0.00004
Flowing O ₂ , 70 ks	0.0003	0.0002
Flowing O ₂ , 50 ks		
yellow-green area	0.0009	0.001
black upper area	0.0004	0.0003
<u>Resistive heating</u>		
Flowing O ₂ , 40 ks		
yellow-grey front		0.005
green back	0.0014, average	0.002

TABLE III

Measured Emittance of TD NiCr

Conditions (All 1100°C and 130 Nm ⁻² , except as noted)	Color of Surface	Emittance at Temps. Noted (800°C, relative)
4 hr. O ₂	Black Grey	0.88 (assumed) 0.86
4 hr. 0·+O ₂	Dark Green Yellow	0.89 0.75

		(1100°C, absolute)*
Unoxidized, vacuum	Bare metal	0.33
Flowing O ₂ , 600 s	Black/grey	0.88
Flowing O ₂ , 4 ks	Black/grey	0.925
Then,		
Flowing 0·+O ₂ , 600 s	Grey	0.88
Flowing 0·+O ₂ , 3 ks	Yellow-grey	0.82
Flowing 0·+O ₂ , 11 ks	Yellow-grey	0.75 to .78
Flowing 0·+O ₂ , 26 ks	Yellow-grey	.60

* Readings are not corrected for absorptance of quartz; true values are about 5% lower.

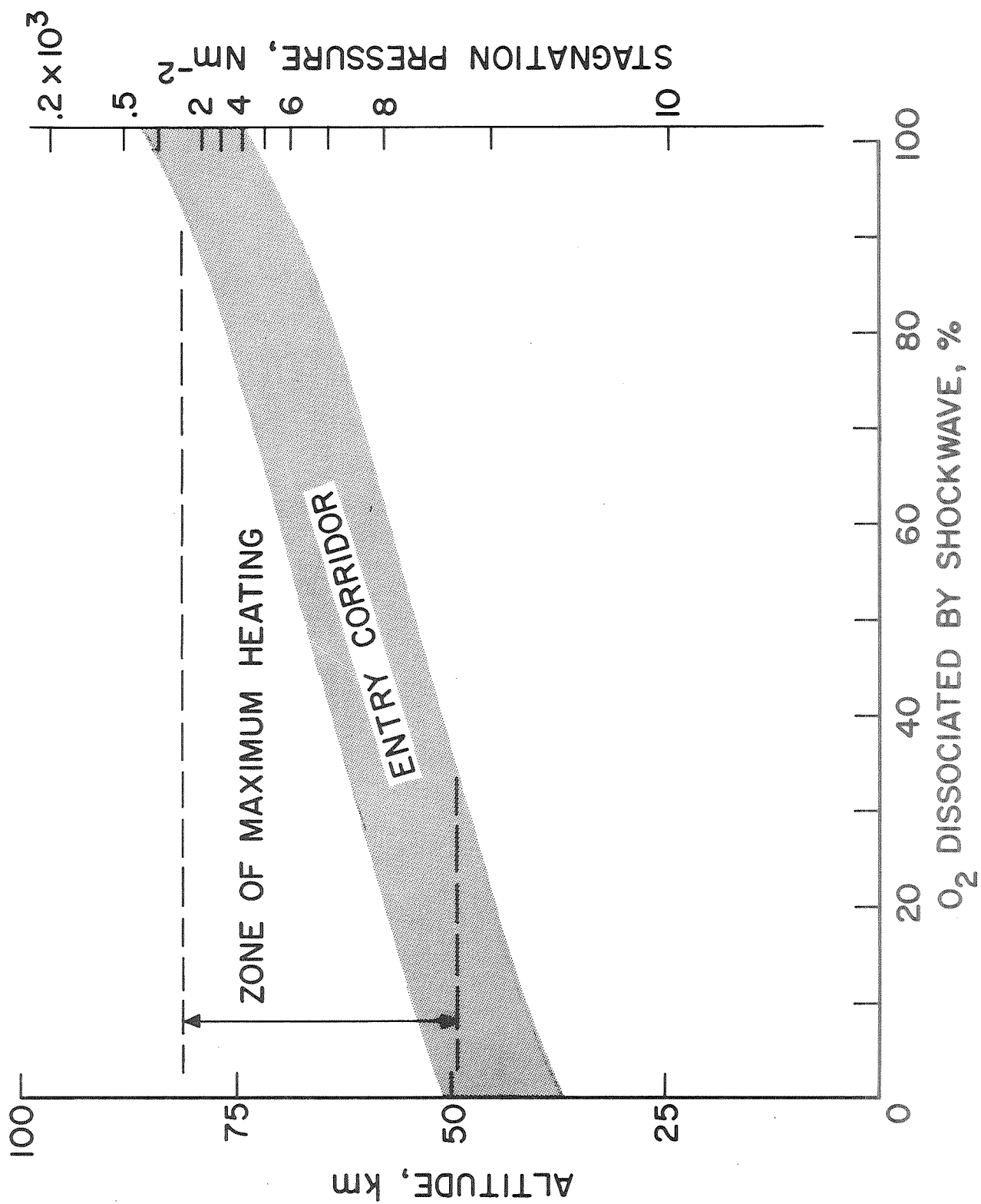


Fig. 1. - Shuttle orbital vehicle reentry environment for a 30° attack.

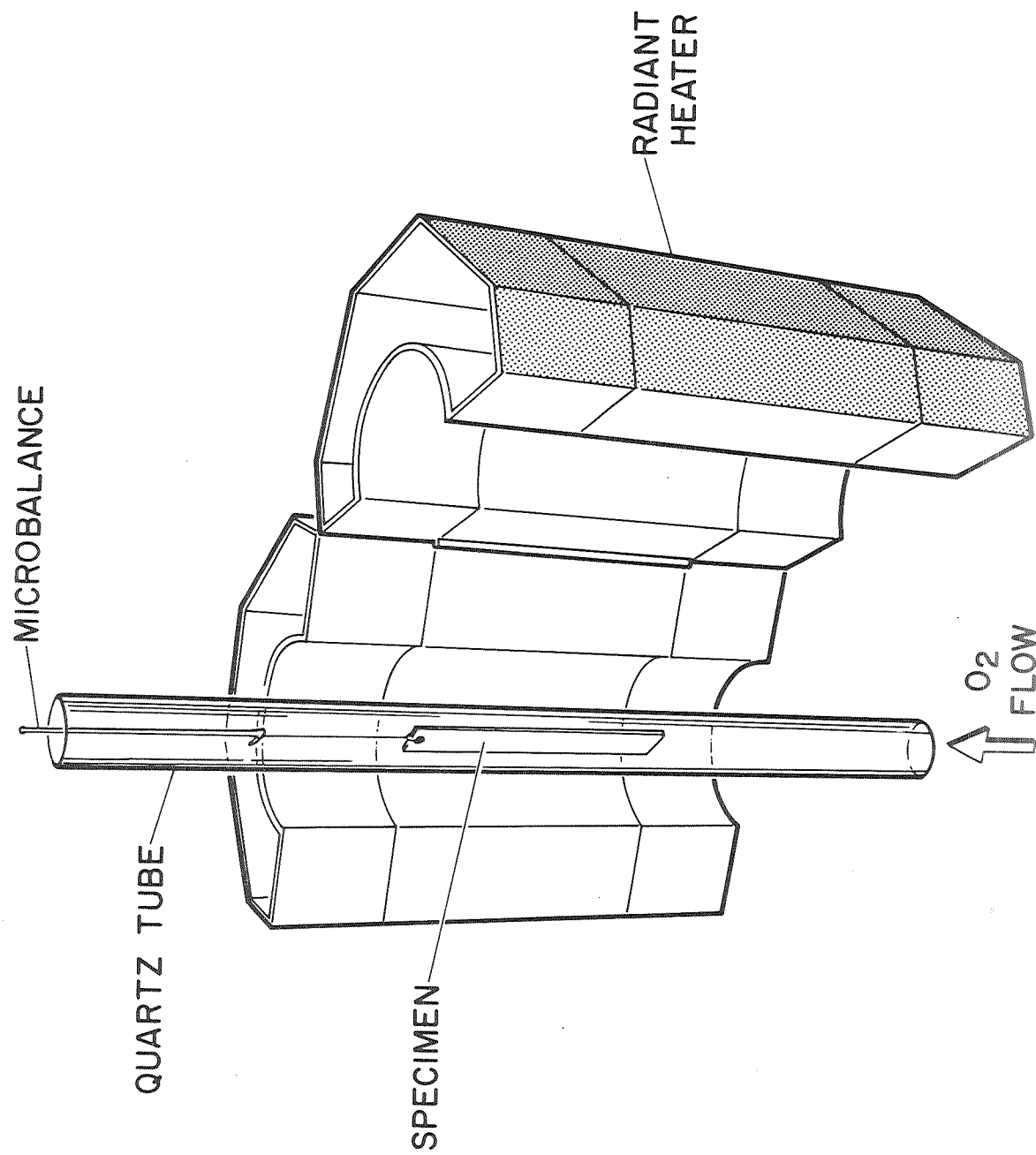


Fig. 2. - Schematic of apparatus for radiantly heating specimens.

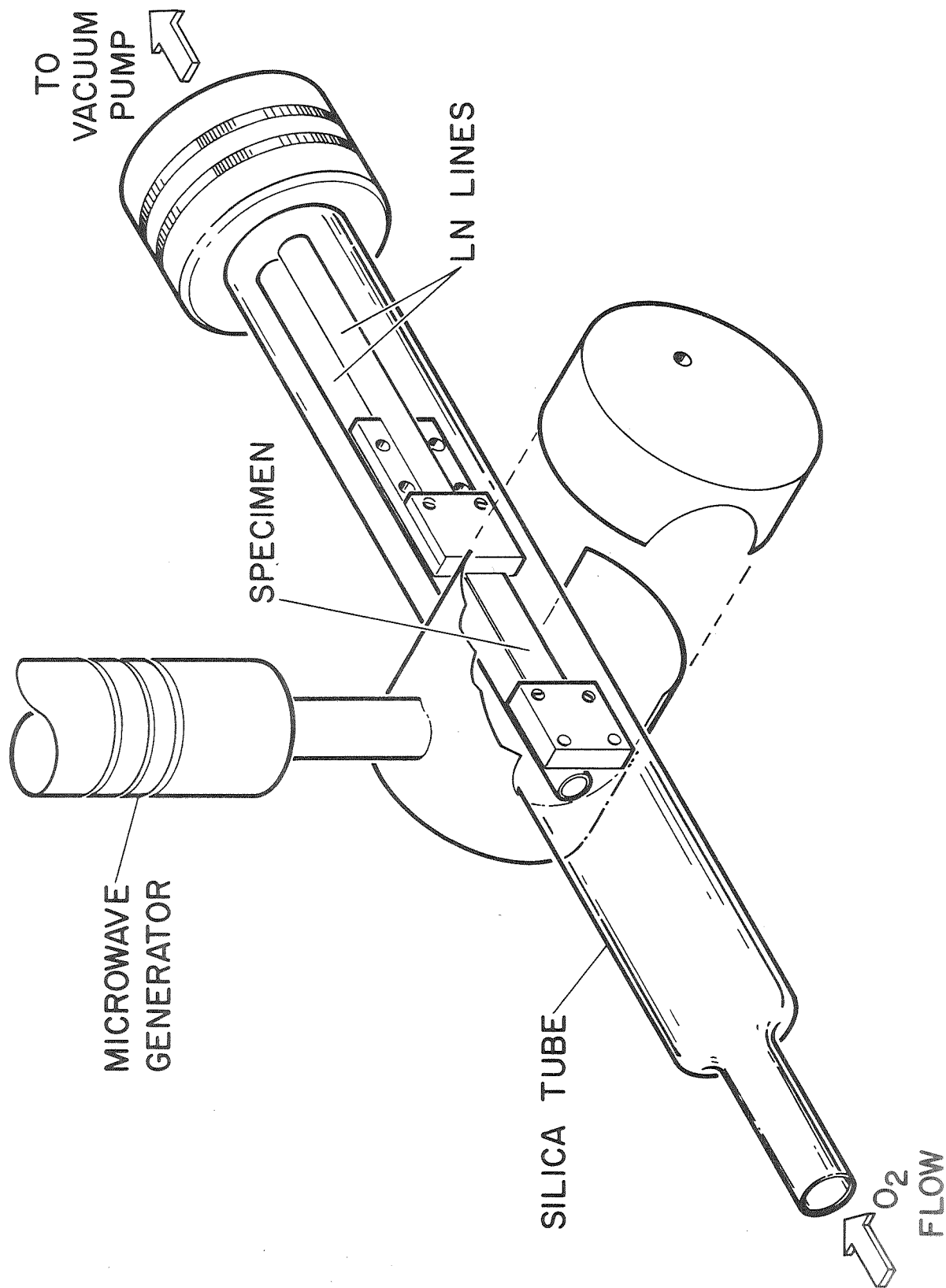


Fig. 3. - Schematic of apparatus for resistively heating specimens.

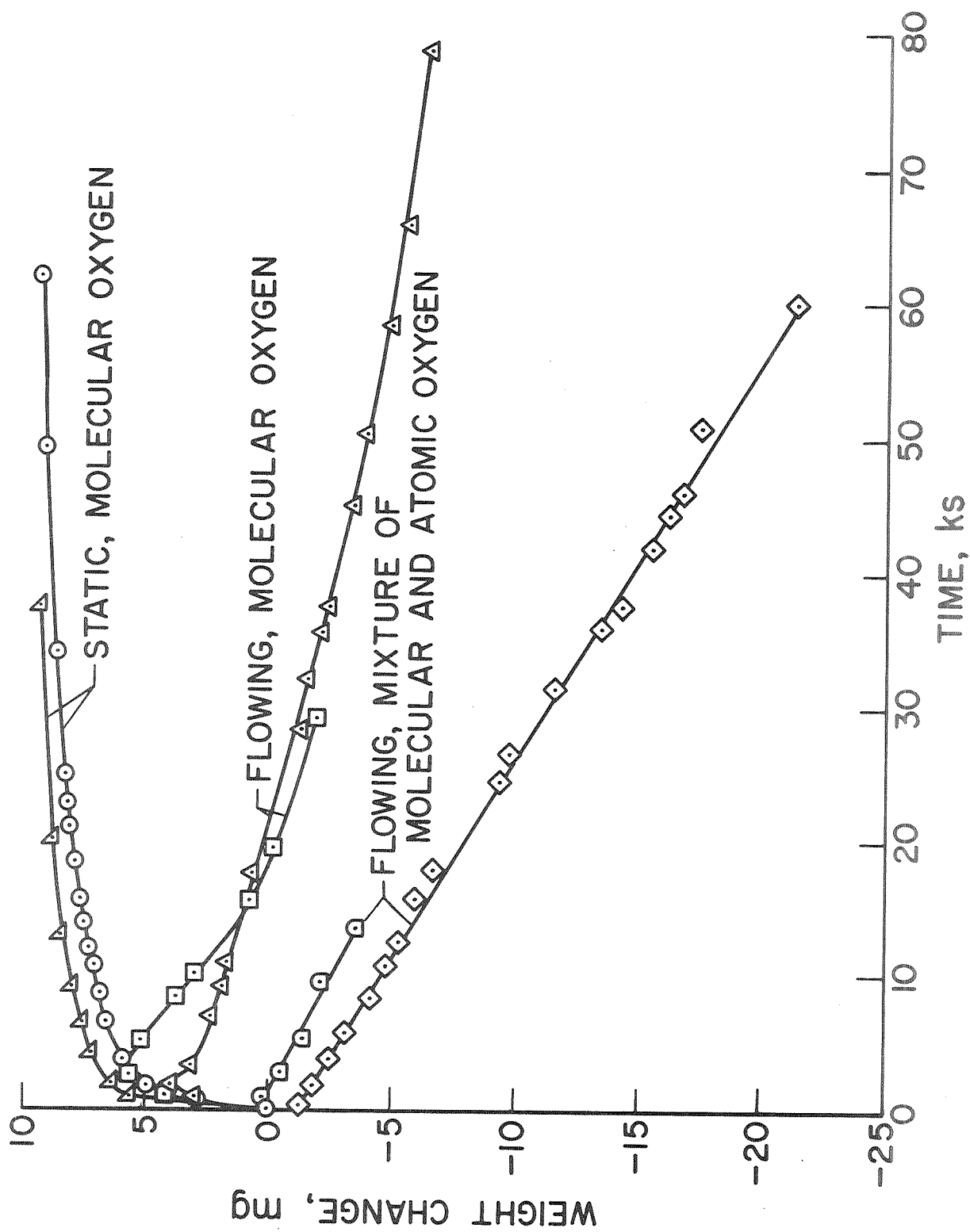


Fig. 4. - Oxidation of TD NiCr specimens (25 cm^2) at 1100°C and 130 Nm^{-2} .